Available online at www.sciencedirect.com
ScienceDirect
Journal of Magnetic Resonance 182 (2006) 293–297
JMR Journal of Magnetic Resonance
www.elsevier.com/locate/jmr

Sensitivity optimization in amplitude-modulated CW-EPR experiment

Matvey Fedin [a,*], Igor Gromov [b], Arthur Schweiger [b,✠]

[a] International Tomography Center SB RAS, Novosibirsk 630090, Russia
[b] Physical Chemistry Laboratory, ETH Zurich, 8093 Zurich, Switzerland

Received 21 April 2006; revised 10 July 2006
Available online 27 July 2006

Abstract

A sensitivity of recently developed method of amplitude-modulated continuous wave EPR (AM-CW-EPR) is studied depending on the parameters of the modulation field. The case of the significant saturation and high modulation frequency is addressed. It is found, that the rapid resonance passage effect is essential for AM-CW-EPR. However, its manifestation is different comparing to the conventional CW-EPR experiment. Both experimental data and numerical simulations support the enhancement of the AM-CW-EPR sensitivity under the rapid passage conditions for the modulating magnetic field, which is important for practical use of the method.

Keywords: Electron paramagnetic resonance; EPR; ESR; Modulation; Absorption line shapes; Saturation; Multiple-photon transitions

1. Introduction

A new type of the continuous wave EPR (CW-EPR) experiment has been proposed recently [1]. In conventional CW-EPR a modulation of the magnetic field is used in order to increase the sensitivity. The disadvantage of using the modulation is the derivative-like shape of the detected spectra, which results in the dependence of sensitivity on the width of the spectral lines. In recently developed method of amplitude-modulated CW-EPR (AM-CW-EPR) the absorption line shapes of the broad inhomogeneous EPR lines are measured, and thus the sensitivity for this case can be improved.

AM-CW-EPR employs the different modulation scheme comparing to the conventional CW-EPR. The modulation signal is described by the function $A_{\mathrm{am}}(t)\cos(\omega_{\mathrm{rf}}t+\varphi)$, where ω_{rf} is the frequency of field modulation and φ is its phase, $A_{\mathrm{am}}(t)$ is the step function (1/0) with period $T=2\pi/\omega_{\mathrm{am}}$, and ω_{am} is the amplitude-modulation frequency (Fig. 1). The phase sensitive detection (PSD) is carried out at frequency ω_{am}. In conventional CW-EPR the 100 kHz modulation frequency is most often used, which coincides with the PSD reference frequency. In AM-CW-EPR the amplitude-modulation frequency ω_{am} and PSD reference frequency are set to 100 kHz, while for the carrier frequency ω_{rf} the values between 200 and 400 kHz and several MHz can be used. A disadvantage of AM-CW-EPR is the necessary requirement to reach at least slight saturation of spectral lines, which can be done by carrying the experiments at low temperatures or by using the high microwave power.

The physics behind AM-CW-EPR is well understood using the formalism of multiple-photon transitions, which was applied for EPR experiments in a recent series of works [2–6]. It was shown that the well-known intermodulation sidebands observed in CW-EPR when the modulation frequency exceeds the linewidth, originate from the multiple-photon transitions of type $\sigma_{\mathrm{mw}}+k\pi_{\mathrm{rf}}$ ($k\in\mathbf{Z}$). During this process one photon σ_{mw} is absorbed from the transverse microwave field, and an arbitrary number of π_{rf} photons are simultaneously absorbed from the longitudinal oscillating field. The saturation of different order (k) multiple-photon transitions may be significantly different. This difference and the use of the amplitude modulation result in recording the absorption spectra.

* Corresponding author. Fax: +7 383 3331399.
E-mail address: mfedin@tomo.nsc.ru (M. Fedin).
✠ Deceased on January 4, 2006.

1090-7807/$ - see front matter © 2006 Elsevier Inc. All rights reserved.
doi:10.1016/j.jmr.2006.07.008

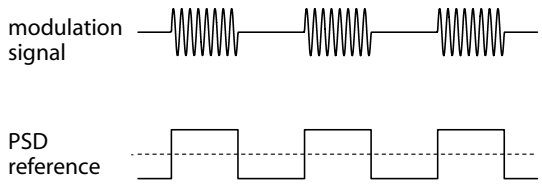

Fig. 1. Scheme for the AM-CW-EPR experiment. Typical modulation signal (top) and corresponding reference signal of phase sensitive detector (bottom).

The main characteristics of AM-CW-EPR experiment were studied in Ref. [1], with the most attention paid to the slight saturation conditions. However, a sensitivity of the method grows up on increase of the saturation, therefore in this work we study the optimum sensitivity conditions under significant saturation. As the sensitivity of AM-CW-EPR depends on the modulation frequency, we discuss the relevance of the rapid resonance passage effects in AM-CW-EPR. Rapid passage occurs when the rate of change of magnetic field is greater than the electron spin relaxation rate [7–9]. In conventional CW-EPR it leads to the distortion of the line shape and to the phase lag with respect to the modulation, however these factors can be used for the strong sensitivity enhancement [10,11]. The manifestations of the rapid passage effects in AM-CW-EPR are found to be different and important for the sensitivity optimization.

2. Experimental

The experimental setup was described in Ref. [1]. The amplitude-modulated longitudinal field was produced by a pulse ENDOR probe head rotated by 90° around its axis, and the detection was carried out using a built-in phase sensitive detector of the commercial X-band EPR spectrometer Bruker Elexsys E580. The relaxation times were measured at the same spectrometer in a pulse mode. Following Ref. [1], the powder sample of ^{63}Cu(II)-doped bis(salicylaldoximate)Ni(II) (Ni(sal)$_2$) with a Cu(II) concentration of about 1% [12] was used.

During the AM-CW-EPR experiments, the microwave absorption is always measured. Note, that unlike in standard CW-EPR, the microwave dispersion cannot essentially contribute to the AM-CW-EPR signal at significant saturation. This happens because the zeroth harmonic of the dispersion signal with respect to ω_{rf} has an antisymmetric shape, resulting in zero integral over the dispersion signal.

3. Results and discussion

Similar to the conventional CW-EPR, the sensitivity of AM-CW-EPR depends on the amplitude of the mw field $2\omega_1$ and on the amplitude of the modulating field $2\omega_2$. In addition, the sensitivity depends on the frequency of the modulating field ω_{rf}. Analytical description of the CW-EPR with account of field modulation is developed only for the case of small saturation parameter $S = \omega_1^2 T_1 T_2 \ll 1$, where T_1 and T_2 have their usual meanings of the longitudinal and transverse relaxation times, respectively [13]. The cases of intermediate and strong saturation are to be considered numerically. This takes place for the AM-CW-EPR as well: the analytical expressions can only be obtained for $S \ll 1$. Based on expression (61) of Ref. [3], the AM-CW-EPR spectrum of individual homogeneous line can be written as

$$P = \sum\nolimits_{k=-\infty}^{\infty} \left[\frac{\omega_1 T_2 J_k^2(z)}{1 + \omega_1^2 T_1 T_2 J_k^2(z) + (\Omega_S - k\omega_{rf})^2 T_2^2} - \frac{\omega_1 T_2 J_k^2(0)}{1 + \omega_1^2 T_1 T_2 J_k^2(0) + (\Omega_S - k\omega_{rf})^2 T_2^2} \right], \quad (1)$$

where $z = 2\omega_2/\omega_{rf}$ and $J_k(z)$ is the Bessel function of the first kind and order k. This expression was obtained using the toggling frame approach [3] and an additional condition $\omega_1/\omega_{rf} \ll 1$. However, very close approximate solution was obtained for arbitrary ratio ω_1/ω_{rf} in Ref. [1]. The AM-CW-EPR spectrum of individual homogeneous line consists of a number of lines spaced with the ω_{rf} (1), and the spectrum of inhomogeneous line is obtained by a convolution over all homogeneous lines. Therefore, the sensitivity of AM-CW-EPR is defined as $I = \int_{-\infty}^{\infty} P \, d\Omega_S$ and can be evaluated for $S \ll 1$ as [1]

$$I \approx \pi \omega_1 S \left[1 - \sum_{k=-\infty}^{\infty} J_k^4(z) \right]. \quad (2)$$

Thus, the sensitivity of AM-CW-EPR increases with the increase of the saturation parameter S, which was also found experimentally [1]. While for $S \ll 1$ the dependence of sensitivity on ω_1, ω_2 and ω_{rf} is clearly described by Eq. (2), it becomes much more complex under conditions $S \sim 1$ or $S > 1$, where the method is best operative.

Fig. 2A shows the experimentally measured dependence $I(\omega_1)$ on ^{63}Cu(II)-doped Ni(sal)$_2$ powder sample for the fixed value of $z = 2\omega_2/\omega_{rf} = 0.7$ and two different values $\omega_{rf} = 1$ and 4 MHz. The value I was measured as the amplitude of the AM-CW-EPR spectrum at ~330 mT (inset). According to Eq. (2), for small values of S the curves $I(\omega_1)$ should coincide for the same z. However, one can see that for significant saturation $I(\omega_1)$ depends not only on the ratio $z = 2\omega_2/\omega_{rf}$, but also separately on ω_{rf}. For higher values of ω_{rf} the significantly higher sensitivity is achieved. In addition, the maximum of the saturation curve $I(\omega_1)$ shifts towards the higher values of ω_1 (lower attenuation values). Fig. 3A shows the dependence $I(\omega_{rf})$ for the fixed $z = 0.7$ and ω_1 (corresponding to 20 dB mw power attenuation) measured at $T = 140$, 110 and 80 K. An increase of the sensitivity with ω_{rf} is observed for all three temperatures. The absolute values of I are higher at lower temperatures, as relaxation times increase leading to an increase of the saturation parameter S.

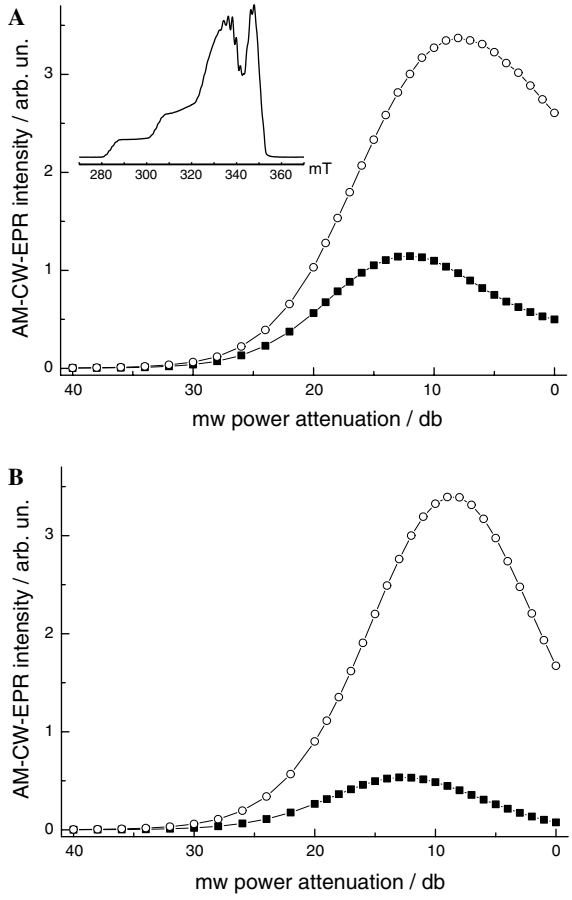

Fig. 2. (A) Experimentally obtained AM-CW-EPR signal intensity at $T = 80$ K as a function of the mw power attenuation. $\omega_{rf} = 1$ MHz (squares) and $\omega_{rf} = 4$ MHz (circles); $z = 0.7$. Inset: the AM-CW-EPR spectrum of ^{63}Cu(II)-doped Ni(sal)$_2$ powder sample. (B) Simulated AM-CW-EPR signal intensity. The parameters used are $T_1 = 6.47$ μs, $T_2 = 215$ ns, $z = 0.7$, $\omega_{rf} = 1$ MHz (squares) and $\omega_{rf} = 4$ MHz (circles).

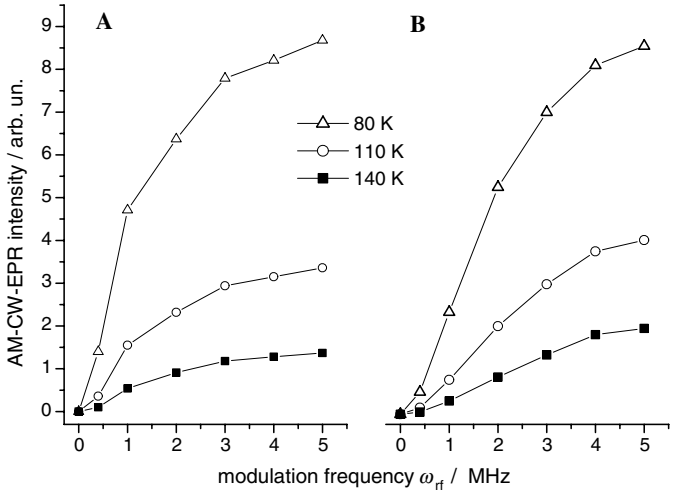

Fig. 3. (A) Experimentally obtained AM-CW-EPR signal intensity as a function of ω_{rf} at $T = 80$, 110 and 140 K; $z = 0.7$. (B) Simulated AM-CW-EPR signal intensity. The parameters used are: 80 K, $T_1 = 6.47$ μs, $T_2 = 215$ ns; 110 K, $T_1 = 3.06$ μs, $T_2 = 139$ ns; 140 K, $T_1 = 1.57$ μs, $T_2 = 108$ ns; $z = 0.7$.

The increase of the sensitivity occurring with an increase of ω_{rf} is an important characteristic of the AM-CW-EPR which was not considered in Ref. [1]. We have shown previously, that even using relatively small values of $\omega_{rf} = 400$ kHz to 1 MHz one can obtain the sensitivity improvement of an order of magnitude comparing to the conventional CW-EPR [1]. This range of ω_{rf} is recommended when the standard CW-EPR cavities are in use with the modulation coils separated from the sample by a thin metal wall. At higher values of ω_{rf} the modulation amplitude ω_2 produced at the sample position is significantly decreased due to the skin-effect, therefore reasonable ω_2 values require very large electric current to be fed to the coils. However, using an ENDOR probe head rotated by 90° over its axis enables one to produce the modulation with ω_{rf} on the MHz scale and thus increase the sensitivity furthermore. Therefore, the dependence $I(\omega_{rf})$ has to be studied in more detail.

The increase of sensitivity with ω_{rf} and the failure of Eq. (2) to describe this behavior for the fixed z can possibly have two qualitative explanations. (i) The first one is that when ω_1 becomes comparable to or higher than ω_{rf} each multiple-photon transition cannot be considered separately and toggling frame approach is not applicable. Therefore, for $\omega_1 \sim \omega_{rf}$ the interference (overlap) of the different-order multiple-photon transitions occurs leading to a decrease of the sensitivity. At $\omega_{rf} > \omega_1$ this interference decreases and disappears at significantly high values ω_{rf}, in agreement with the shapes of the curves shown in Fig. 3A. (ii) The second possible explanation of the dependence $I(\omega_{rf})$ is related to the rapid passage effects. As was mentioned above, rapid passage occurs when the rate of change of magnetic field is greater than the electron spin relaxation rate. Therefore, an increase of ω_{rf} can lead to an increase of the contributions from the rapid passage effects. When the magnetic field is changed too fast comparing to the relaxation rates, the magnetization vector remains closely parallel to the rotating field $\vec{B}_0 + \vec{B}_1$ and does not follow the effective magnetic field $\vec{B}_{eff} = \vec{B}_0 + \vec{B}_1 + \vec{B}_2 \cos(\omega_{rf} t)$ due to the relaxation ($B_1 = \omega_1/\gamma_e$, $B_2 = 2\omega_2/\gamma_e$) [10]. This should influence the amplitude of each multiple-photon transition forming the AM-CW-EPR spectrum of individual homogeneous line. For example, the absorption of the mw power at the central band may be hindered due to the rapid passage when the modulation with a frequency ω_{rf} is switched on. During the other half of the amplitude-modulation cycle, when $\omega_{rf} = 0$, the absorption of the mw power is identical to the case of slow passage conditions. In a way, the amplitude modulation may work as a switch between rapid and slow passage conditions. Therefore, the AM-CW-EPR may be sensitive to the effects analogous to the effect of rapid passage, i.e. to the ratio between ω_{rf}, ω_2 and the relaxation times T_1 and T_2.

In order to understand which of the two explanations above is relevant for the experimentally observed dependence $I(\omega_{rf})$, the simulations have been done. The numerical solution of the Bloch equations has been performed

taking account of the modulation signal shape and PSD reference signal relevant for AM-CW-EPR experiment (Fig. 1). Fig. 4A shows the calculated dependence $I(\omega_{rf})$ for different ratios between ω_1, T_1 and T_2. Each point of the curve $I(\omega_{rf})$ corresponds to the integral over the calculated spectrum of the individual homogeneous line. The shapes of all obtained dependences resemble the experimental curves in Fig. 3A, the growth of the sensitivity with ω_{rf} is observed. The increase of the ω_1 by a factor of two ($\omega_1' = 2\omega_1$, saturation factor $S' = 4S$) results in a most pronounced growth of the absolute values of I. This agrees with the expression (2), as $I \propto \omega_1 S \propto \omega_1^3$ (not simply $I \propto S \propto \omega_1^2$). The increase of the T_1 in four times ($T_1' = 4T_1, S' = 4S$) results in less pronounced growth of the absolute values of I. However, both normalized curves coincide and are slightly different from the curve calculated for ω_1, T_1, S (Fig. 4B). This means, that the parameters ω_1 and T_1 do not influence the shape of the $I(\omega_{rf})$ curve significantly. The most pronounced difference in the shape of the dependence $I(\omega_{rf})$ is found when the transverse relaxation time T_2 is increased by a factor of 4 ($T_2' = 4T_2, S' = 4S$). The growth of the sensitivity at low values of ω_{rf} is very steep, and the plateau of the dependence $I(\omega_{rf})$ is reached much faster than in all other cases. In the opposite case when $T_2' = T_2/4, S' = S/4$, the growth of the $I(\omega_{rf})$ curve is much slower and it does not approach the plateau at $\omega_{rf} < 10$ MHz. Therefore, we conclude, that the observed shape of the dependence $I(\omega_{rf})$ is mainly determined by the ratio between ω_{rf} and $1/T_2$. This means, that the observed growth of the sensitivity on ω_{rf} is caused by the rapid resonance passage due to the modulation of longitudinal field. Resuming, the sensitivity of AM-CW-EPR can be increased significantly by fulfilling the condition $\omega_{rf} T_2 > 1$.

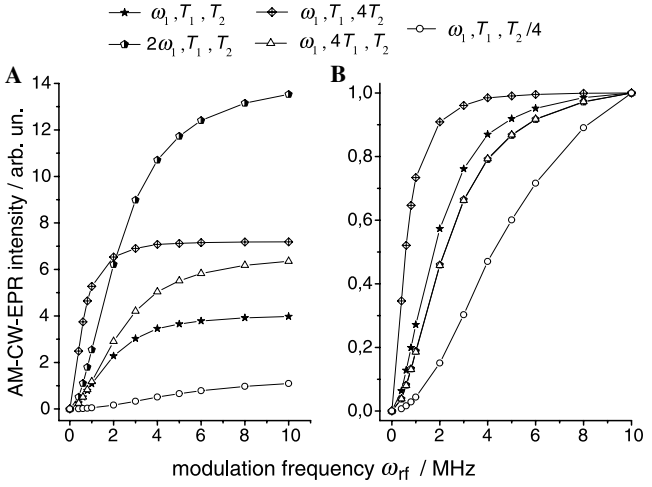

Fig. 4. Simulated AM-CW-EPR signal intensity as a function of ω_{rf} for various ratios between relaxation times and mw field amplitude. (A) The curves are shown on the same scale, (B) the curves are normalized. Various values of $\omega_1' = c_0\omega_1, T_1' = c_1 T_1$ and $T_2' = c_2 T_2$ are given in the legend, respectively, where $c_{0,1,2}$ are the constants, $\omega_1 = 1$ MHz, $T_1 = 5$ μs, $T_2 = 200$ ns; $z = 1$.

The values for the relaxation times T_1 and T_2 used in model simulations in Fig. 4 are very close to the real ones for the ^{63}Cu(II)-doped Ni(sal)$_2$ sample. The phase memory time T_m was measured as an exponential decay time of a two-pulse electron spin echo intensity on an increase of the pulse separation time (Fig. 5A). The obtained values for the spectral position $B_0 = 330$ mT are 108, 139 and 215 ns (±5 ns) at temperatures $T = 140$, 110 and 80 K, respectively, and can be associated with a transverse

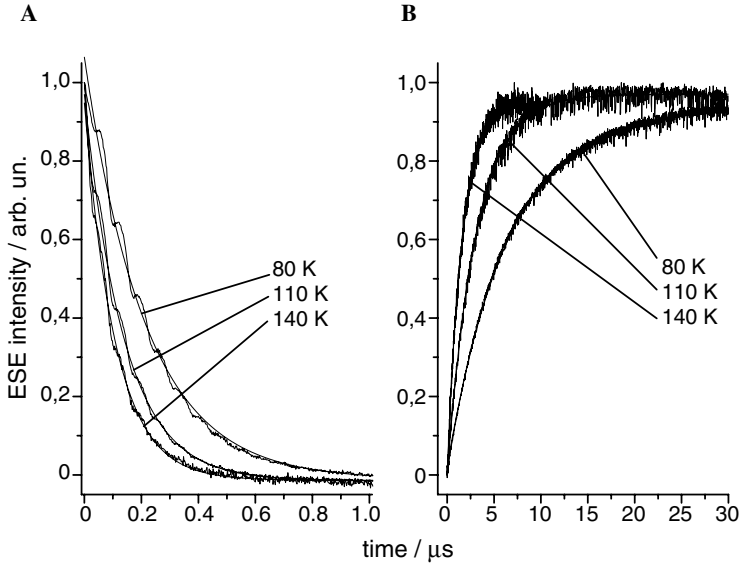

Fig. 5. (A) The measurement of T_m: two-pulse electron spin echo intensity as a function of the interpulse time delay. $B_0 = 330$ mT, π/2-pulse length of 20 ns is used. (B) The measurement of T_1: saturation-recovery sequence is used. High power saturation pulse of 8 μs length is followed by a two-pulse detection sequence π/2–τ–π with the length of π/2-pulse of 20 ns. The time delay between the saturation pulse and the detection sequence is incremented, $B_0 = 330$ mT.

relaxation time T_2. The longitudinal relaxation time T_1 was measured using a saturation-recovery sequence and have the values 1.57, 3.06 and 6.47 μs (±0.1 μs) at $T = 140$, 110 and 80 K, respectively (Fig. 5B). As for many solids, the phase memory time in this range of temperatures varies much less than the spin–lattice relaxation time T_1. The change of the experimentally observed dependence $I(\omega_{rf})$ with temperature is indeed consistent with a change driven mostly by the increase of T_1. The curves in Fig. 3B were calculated by adjusting only the ω_1 value (the same for all curves) and using the above relaxation times, and are in good agreement with the experiment in Fig. 3A: both the curve shapes and the relative amplitudes are reproduced. The dependence $I(\omega_1)$ calculated using the same parameters changes with ω_{rf} in a good agreement with experiment (Fig. 2B). The calculated increase of the amplitude of $I(\omega_1)$ dependence between $\omega_{rf} = 1$ and 4 MHz exceeds the experimental one (Fig. 2A), however the slight shift of the maximum of $I(\omega_1)$ is very well reproduced. Thus, the numerical simulations essentially reproduce all the observed phenomena.

It is typical for the solids that $T_2 \ll T_1$ and thus the situation modeled by ^{63}Cu(II)-doped Ni(sal)$_2$ applies for the most of the practical situations. Therefore, for many samples of interest the sensitivity of AM-CW-EPR can be strongly increased by increasing the high modulation frequency ω_{rf}. Of course, the spectral resolution in this case cannot exceed $2\omega_{rf}$, and hence the optimum value has to be chosen [1]. However, for the broad EPR lines where AM-CW-EPR is superior to the conventional CW-EPR, the resolution of several gauss allows one to use the ω_{rf} values up to several MHz.

4. Conclusions

The AM-CW-EPR is an alternative method of measuring absorption EPR spectra in CW mode. It has a superior sensitivity compared to a conventional CW-EPR for broad inhomogeneous EPR lines, which was discussed in detail in Ref. [1]. The drawback of AM-CW-EPR is the necessity of achieving at least slight saturation conditions. The advantage is that only a small modification of standard CW-EPR setup is required. In this work, we have studied the conditions for the modulation field when the sensitivity of AM-CW-EPR can be increased furthermore. This occurs upon an increase of the high modulation frequency ω_{rf} due to the rapid resonance passage effects. Although the values of ω_{rf} achieved using the modulation coils of standard CW-EPR cavity are limited to ca. 1 MHz, the use of the ENDOR setup allows one to create the ω_{rf} of several MHz and higher. The experimentally observed sensitivity improvement by adjusting the ω_{rf} value was up to 6 times at $\omega_{rf} = 400$ kHz to 5 MHz for the copper complex studied. Therefore, the results of this work can be helpful for the practical use of AM-CW-EPR and for optimization of its sensitivity.

Acknowledgments

This work was supported by INTAS (YSF 04-83-2669) and RFBR (05-03-32264-a) and by Swiss National Foundation.

References

[1] M. Fedin, I. Gromov, A. Schweiger, Absorption line CW EPR using an amplitude modulated longitudinal field, J. Magn. Reson. 171 (2004) 80.
[2] I. Gromov, A. Schweiger, Multiphoton transitions in pulse EPR, J. Magn. Reson. 146 (2000) 110.
[3] M. Kälin, I. Gromov, A. Schweiger, The continuous wave electron paramagnetic resonance experiment revisited, J. Magn. Reson. 160 (2003) 166.
[4] M. Kälin, I. Gromov, A. Schweiger, Transparency in two-level spin systems induced by a longitudinal field, Phys. Rev. A 69 (2004) 033809.
[5] M. Fedin, M. Kälin, I. Gromov, A. Schweiger, Applications of π-photon-induced transparency in two-frequency pulse electron paramagnetic resonance experiments, J. Chem. Phys. 120 (2004) 1361.
[6] M. Kälin, M. Fedin, I. Gromov, A. Schweiger, Multiple-photon transitions in EPR spectroscopy, Lect. Notes Phys. 684 (2006) 143.
[7] A.M. Portis, Rapid passage effects in electron spin resonance, Phys. Rev. 100 (1955) 1219.
[8] J.S. Hyde, Magnetic resonance and rapid passage in irradiated LiF, Phys. Rev. 119 (1960) 1483.
[9] M. Weger, Passage effects in paramagnetic resonance experiments, Bell. Syst. Tech. J. 39 (1960) 1013.
[10] C. Mailer, C.P.S. Taylor, Rapid adiabatic passage EPR of ferricytochrome c: signal enhancement and determination of the spin–lattice relaxation time, Biochim. Biophys. Acta 232 (1973) 195.
[11] J.R. Harbridge, G.A. Rinard, R.W. Quine, S.S. Eaton, G.R. Eaton, Enhanced signal intensities obtained by out-if-phase rapid-passage EPR for samples with long electron spin relaxation times, J. Magn. Reson. 156 (2002) 41.
[12] E.G. Cox, F.W. Pinkard, W. Wardlaw, K.C. Webster, Planar configuration for guadricovalent nickel, palladium and platinum, J. Chem. Soc. (1935) 459.
[13] O. Haworth, R.E. Richards, The use of modulation in magnetic resonance, in: J.W. Emsley, J. Feeney, L.H. Sutcliffe (Eds.), Progress in Nuclear Magnetic Resonance Spectroscopy, vol. 1, Pergamon, New York, 1966, p. 1.